Electrochimica Acta 213 (2016) 641–647

Contents lists available at ScienceDirect

Electrochimica Acta

journal homepage: www.elsevier.com/locate/electacta

H_xMoO_3 nanobelts with better performance as anode in lithium-ion batteries

Xiaokang Ju, Peigong Ning, Xiaobing Tong, Xiaoping Lin, Xi Pan, Qiuhong Li,
Xiaochuan Duan*, Taihong Wang*

Pen-Tung Sah Institute of Micro-Nano Science and Technology, Xiamen University, Xiamen 361005, China

ARTICLE INFO

Article history:
Received 6 June 2016
Received in revised form 27 July 2016
Accepted 31 July 2016
Available online 1 August 2016

Keywords:
H_xMoO_3
anode
high rate
Lithium-ion batteries

ABSTRACT

We first report the pure H_xMoO_3 nanobelts as anode for lithium-ion batteries by a facile hydrothermal with ammonium heptamolybdate tetrahydrate ($(NH_4)6Mo_7O_{24}\cdot 4H_2O$) and hydrochloric acid (HCl). Owing to hydrogen-doping, Mo^{5+} exists in the H_xMoO_3 nanobelt, which may release extra electrons. Therefore, the electric conductance of H_xMoO_3 nanobelt is enhanced greatly. Moreover, the content of hydrogen can't be high, since the ordered structure deteriorates when amount of hydrogen increasing. The $H_{0.28}MoO_3$ nanobelts we designed exhibit outstanding specific capacity and rate performance. The stable capacity of 920 mAh g^{-1} is obtained after 25 charge/discharge cycles at 100 mA g^{-1}. At high current densities such as 1, 2, 5 and 10 A g^{-1}, the $H_{0.28}MoO_3$ electrode delivers specific capacities of about 600, 500, 420, 300 mAh g^{-1}, respectively. Even after 450 charge discharge cycles at 1 A g^{-1}, the performance of our materials can maintain the capacity of about 550 mAh g^{-1}. Furthermore, we provide more discussion about the lithium storage mechanism of H_xMoO_3 nanobelts through ex situ XRD and FESEM. By comparing H_xMoO_3 with different X, we find that low content of hydrogen can greatly improve the performance of α-MoO_3 electrodes in Li-ion batteries.

1. Introduction

Lithium-ion batteries (LIBs) have been widely used in various fields, such as mobile phones, laptops, and other small portable appliances [1–4]. In addition, significant improvements in rate and endurance for economic, safe electrode materials may make possible utilization in plug-in hybrid electric vehicles (PHEVs) [4–8]. Great effort has been made to develop graphite alternatives, which deliver higher specific capacity than 372 mAh g^{-1}. A good anode material candidate should be characterized by a high specific capacity, a highly reversible Li insertion/de-insertion as well as low polarization [9–21].

Recent work has been concentrated on preparing nanostructures for improving capacity and rate index in LIBs electrode [22]. The morphology of 1D material has not only enlarged electrode-electrolyte contact areas and relaxed strain of volume expansion, but also provided efficient 1D electron transport pathways [23]. Orthorhombic molybdenum trioxide (α-MoO_3) exhibits a characteristic double-layered structure consisting of MoO_6 octahedron units with lattice constants a = 3.962 Å, b = 3.855 Å, and c = 3.699 Å [24]. Orthorhombic crystal structure is based on a series of bilayers which should be perpendicular to the [010] axis. [25]. This unique characteristic makes it be one of the most potential candidates to form large surface areas and high surface-to-volume ratio nanostructures [26]. In this paper, we employed a one-step hydrothermal approach to synthesize the 1D nanobelts MoO_3 and H_xMoO_3. The theoretical specific capacity of MoO_3 is about 1117 mAh g^{-1}, which is nearly three times that of graphite. However, its applications have been limited by its poor electronic conductivity.

Some techniques have been proved to be effective, such as dimensionality reduction, synthesis of MoO_3 nanobelt-graphene composites, ion-doping, coating [16,27–30], and et al., which are being reported in the past few years. The electrochemical reactivity of MoO_3/C as anode material has been investigated by Xia et al. [31] and compared with pure MoO_3 electrode, MoO_3/C exhibits much higher specific capacity (a stable capacity of 600 mAh g^{-1} is delivered at 100 mA g^{-1}) due to the protection of carbon layer. In another study [32], SnO_2/MoO_3/C nanostructure delivers a reversible discharge capacity of 500 mAh g^{-1} after 120 cycles at a high current density of 200 mA g^{-1}, because of the 1-D nanostructure composed of nanosheets and the carbon matrix. Great progress in improving capacities of MoO_3 has also been

---

* Corresponding author. Tel.:+86 0592 2187196; fax: +86 0592 2197196.
E-mail address: thwang@xmu.edu.cn (T. Wang).

http://dx.doi.org/10.1016/j.electacta.2016.07.160
0013-4686/

achieved recently. B. Ahmed et al. [33] have coated MoO_3 nanobelts with HFO_2, and the HFO_2-coated nanobelts demonstrates a high capacity of more than 600 mAh g^{-1} at a current density of 1000 mA g^{-1} after 50 cycles. The presence of HFO_2 layer serves as protective barrier at anode/electrolyte interface. Herein, electrode design appears to be a critical issue for meeting the development of LIBs.

In this work, an alternative method of preparing H_xMoO_3 nanobelts is proposed. As a potential candidate of the electron-proton mixed conductor, the hydrogen molybdenum bronze (H_xMoO_3) has drawn more and more attention due to their applications in hydrogen-transfer catalysts, electrochromic displays, fuel cell, integration of nanoscale electronic devices and hydrogen storage [34–37] but rarely focusing on lithium-ion batteries. And as we all know, the transitional metallic cations are shown with mixed valences in H_xMoO_3 nanobelts [37]. Owing to hydrogen-doping, Mo^{5+} exists in the nanobelts, which may release extra electrons that are quasi-free within the MoO_6 octahedral. Therefore, the electric conductance of H_xMoO_3 nanobelt is enhanced greatly. Indeed, there are series of compounds of layered MoO_3 with different hydrogen contents. And the samples are transformed from orthorhombic to monoclinic with the increase of the hydrogen content. Intuitively, the colour of MoO_3 turns blue, and gradually darken [38,39]. We find that only the low hydrogen-doping sample is orthorhombic, which is similar to α-MoO_3 that is a thermodynamically stable phase, while monoclinic MoO_3 (β-type) belongs to metastable phase. So, it is better to obtain H_xMoO_3 with smaller x value. In addition, as reported by Wang et al. [40], H_xMoO_3 belongs to $M_xMoO_3{\bullet}nH_2O$. The most distinguish structural feature of $M_xMoO_3{\cdot}nH_2O$ is a wide one-dimensional tunnel (3.2–3.5 Å in diameter), which should allow lithium-ions free intercalation [41]. Up to now, we have only found that song et al. [34] have reported the H0.6MoO3@C (monoclinic phase) nanobelts in LIBs. However, they can't distinguish which play a more important role between carbon coating and hydrogen doping. Moreover, the hydrogen content may be too high that can distort the structure. The inference also has been proved in the following experiment that low hydrogen-doping may be more useful in LIBs. The reversible capacity of synthetic $H_{0.28}MoO_3$ nanobelts is about 920 mAh g^{-1}, which is approaching the theory capacity of $MoO_{3.}$ When testing at a high rate, the performance of our materials can maintain the capacity of about 550 mAh g^{-1} after 450 cycles at 1 A g^{-1}. Even at 10 A g^{-1}, the capacity can still maintain at around 300 mAh g^{-1}

2. Materials synthesis

All the chemical reagents are analytical grade and they are used without further purification. In a facile hydrothermal synthesis, 0.6 g ammonium heptamolybdate tetrahydrate ($(NH_4)6Mo_7O_{24}{\cdot}4H_2O$) is dissolved in 36 ml deionized water under continuous stirring. After 10 minutes, 2.5 ml hydrochloric acid (HCl) is added to the beaker slowly and stirred for another 5 minutes. Then the homogeneous suspension is transferred to a Teflon-lined autoclave with a capacity of 50 ml and kept inside an electric oven at 160 °C for 15 h. The item is then centrifuged and washed with deionized water for several times and dried under vacuum at around 60 °C. $MoO_3$with white colour is observed. In addition, by increasing the amount of HCl to 3.5 ml and 6.5 ml respectively, we can get the synthesis of $H_{0.28}MoO_3$ nanobelts and $H_{0.33}MoO_3$ nanobelts. (Other preparation conditions are all same).

2.1. Materials characterization

The powder X-ray diffraction (XRD) patterns are recorded on a Panalytical X–pert diffracto meter with Cu–Kα radiation. The morphology and crystal structure are collected by scanning electron microscopy (SEM, Hitachi S4800) and high-resolution transmission electron microscopy (HRTEM, JEM–2100). Raman spectroscopy was performed using a micro-Raman 2000 system (Renishaw, Britain) with a 10 mW laser excitation source of wavelength 633 nm. X-ray photoelectron spectrum (XPS) is carried out in ESCALAB 250 with a monochromatic Al Kα X-ray source ($h\nu$= 1486.6 eV) operating at 150 W, a multichannel plate and delay line detector under a vacuum of ~10^{-9} mbar.

2.2. Electrochemical measurements

The electrochemical tests are performed using a CR2016-type coin cell. Pure lithium foils are used as counter electrodes. The active materials are mixed with carbon black and carboxyl methyl cellulose at a weight ratio of 8: 1: 1, which are dispersed in distilled water and alcohol, then to form a homogeneous slurry. The mixed slurry is tape cast on Cu foil and dried at 80 °C for 12 h under vacuum. The dried foil is cut into circular disks to be used as working electrode. The loading density of working electrode is about 0.9–1.2 mg cm^{-2}. The electrolyte solution is 1 M $LiPF_6$ in ethylene carbonate–dimethyl carbonate–diethyl carbonate (1: 1: 1, in weight percent). A Celgard 2400 microporous polypropylene membrane is used as a separator. The coin-type cells are assembled in an argon filled glovebox with water and oxygen contents of less than 0.5 ppm. Galvanostatic charge/discharge cycling performance is carried out by Land CT 2001 battery tester in the voltage range of 3 V–0.01 V vs. Li^+/Li at 25 °C.

3. Results and discussion

Fig. 1 exhibits the XRD patterns of the obtained $H_{0.33}MoO_3$ samples(phase III), $H_{0.28}MoO_3$ samples (phase II) and MoO_3 samples(phase I). The three patterns in Fig. 1 are similar to each other in general, but there are still subtle differences among them. (For example, the magnified pattern of (040) diffraction peaks for $H_{0.28}MoO_3$ and $H_{0.33}MoO_3$ is shown in Fig. S1) The diffraction peaks of three samples can be well-indexed to different JCPDS cards. In addition, the cell lattices of H_xMoO_3 (X = 0.28 and 0.33) and MoO_3 can be seen in Supporting Information of Table 1. It is easy to discover that the lattice unit is enlarged after hydrogen atoms are doped into MoO_3 [42]. The phase I maintains the pristine phase without evident change and agrees well with the XRD pattern of MoO_3 (JCPDS, no:76-1003, orthorhombic). When increasing HCl to

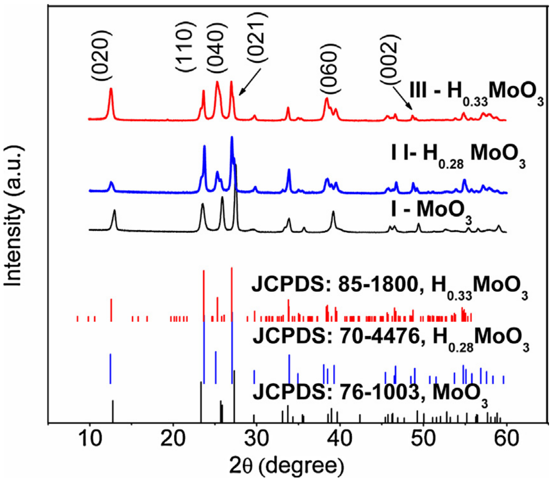

Fig. 1. The XRD patterns of the obtained $H_{0.33}MoO_3$ samples(phase III),$H_{0.28}MoO_3$ samples(phase II) and MoO_3 samples(phase I).